**INTERAGENCY AGREEMENT NO: DE-AIO3-02ER63344**

# PROGRESS REPORT OF FY 2004 ACTIVITIES: IMPROVED WATER VAPOR AND CLOUD RETRIEVALS AT THE NSA/AAO

Principal Investigator: E. R. Westwater[1] 303-497-6527

Co-PIs: V. V. Leuskiy[1], M. Klein[1], A. J. Gasiewski[2], and J. A. Shaw[3]

Institution: [1]CIRES, University of Colorado/
National Oceanic & Atmospheric Administration-Environmental Technology Laboratory

[2]National Oceanic & Atmospheric Administration-Environmental Technology Laboratory

[3]Montana State University

Title: Improved Water Vapor and Cloud Retrievals at the NSA/AAO

SC Division: SC-74

Program Manager: Wanda R. Ferrell 301-903-0043

Research Areas: Water vapor, cloud liquid, microwave radiometers, radiative transfer

# PROGRESS REPORT OF FY 2004 ACTIVITIES: IMPROVED WATER VAPOR AND CLOUD RETRIEVALS AT THE NSA/AAO


## Principal Investigators:

Edgeworth R. Westwater CIRES/NOAA-ETL
Vladimir V. Leuskiy CIRES/NOAA-ETL
Marian Klein, CIRES/NOAA-ETL
Albin J. Gasiewski, NOAA-ETL
Joseph A. Shaw, Montana State University

## Participants

Taneil Uttal, NOAA-ETL
Duane A. Hazen, NOAA-ETL
Domenico Cimini, CIRES
Vinia Mattioli, University of Perugia
Bob L. Weber, STC
Sally Dowlatshahi, STC
James C. Liljegren, ANL
Barry M. Lesht, ANL
B. D. Zak, Sandia NL


## SCIENTIFIC GOALS OF THE RESEARCH

The basic goals of the research are to develop and test algorithms and deploy instruments that improve measurements of water vapor, cloud liquid, and cloud coverage, with a focus on the Arctic conditions of cold temperatures and low concentrations of water vapor. The importance of accurate measurements of column amounts of water vapor and cloud liquid has been well documented by scientists within the Atmospheric Radiation Measurement Program. Although several technologies have been investigated to measure these column amounts, microwave radiometers (MWR) have been used operationally by the ARM program for passive retrievals of these quantities: precipitable water vapor (PWV) and integrated water liquid (IWL). The technology of PWV and IWL retrievals has advanced steadily since the basic 2-channel MWR was first deployed at ARM CART sites Important advances are the development and refinement of the tipcal calibration method [1,2], and improvement of forward model radiative transfer algorithms [3,4]. However, the concern still remains that current instruments deployed by ARM may be inadequate to measure low amounts of PWV and IWL. In the case of water vapor, this is especially important because of the possibility of scaling and/or quality control of radiosondes by the water amount. Extremely dry conditions, with PWV less than 3 mm, commonly occur in Polar Regions during the winter months. Accurate measurements of the PWV during such dry conditions are needed to improve our understanding of the regional radiation energy budgets. The results of a 1999 experiment conducted at the ARM North Slope of Alaska/Adjacent Arctic Ocean (NSA/AAO) site during March of 1999 [5] have shown that the strength associated with

the 183 GHz water vapor absorption line makes radiometry in this frequency regime suitable for measuring low amounts of PWV. As a portion of our research, we conducted another millimeter wave radiometric experiment at the NSA/AAO in March-April 2004. This experiment relied heavily on our experiences of the 1999 experiment. Particular attention was paid to issues of radiometric calibration and radiosonde intercomparisons. Our theoretical and experimental work also supplements efforts by industry (F. Solheim, Private Communication) to develop sub-millimeter radiometers for ARM deployment. In addition to quantitative improvement of water vapor measurements at cold temperature, the impact of adding millimeter-wave window channels to improve the sensitivity to arctic clouds was studied. We also deployed an Infrared Cloud Imager (ICI) during this experiment, both for measuring continuous day-night statistics of the study of cloud coverage and identifying conditions suitable for tipcal analysis. This system provided the first capability of determining spatial cloud statistics continuously in both day and night at the NSA site and has been used to demonstrate that biases exist in inferring cloud statistics from either zenith-pointing active sensors (lidars or radars) or sky imagers that rely on scattered sunlight in daytime and star maps at night [6].

## REFERENCES

[1] Han, Y., and E. R. Westwater, "Analysis and improvement of tipping calibration for ground-based microwave radiometers", *IEEE Trans. Geosci. Remote Sensing*, 38 (3), 1260-1276, 2000.

[2] Liljegren, J. C., "Automatic Self-Calibration of ARM Microwave Radiometers", *Microwave Radiometry and Remote Sensing of the Earth's Surface and Atmosphere*, P. Pampaloni and S. Paloscia Eds., VSP Press, pp. 433-441, 2000.

[3] Liljegren, J. C., S. A. Boukabara, K. Cady-Perteira, and S. Clough, "The Effect of the Half-Width of the 22-GHz Water Vapor Line on Retrievals of Temperature and Water Vapor Profiles with a Twelve-Channel Microwave Radiometer. ", *IEEE Trans. Geosci. Remote Sensing* (in press).

[4] Mattioli ,V. , E. R. Westwater, S. I. Gutman, and V. R. Morris, " Forward Model Studies of Water Vapor using Scanning Microwave Radiometers, Global Positioning System, and Radiosondes during the Cloudiness Inter-Comparison Experiment", *IEEE Trans. Geosci. Remote Sensing* (in press).

[5] Racette, P. E., E. R. Westwater, Y. Han, A. J. Gasiewski, M. Klein, D. Cimini, D. C. Jones, W.Manning, E. J.Kim, J.R. Wang, V. Leuski, P. Kiedron, "Measurement of Low Amounts of Precipitable Water Vapor Using Ground-Based Millimeterwave Radiometry", *J. Atmos. Oceanic Technol.* (in press)

[6] B. Thurairajah and J. A. Shaw. "Cloud statistics measured with the Infrared Cloud Imager," *IEEE Trans. Geosci. Remote Sensing* (submitted).

# MAJOR ACCOMPLISHMENTS DURING THE PERIOD NOVEMBER 1, 2003 to OCTOBER 31, 2004

## 1. 1997, 1998, and 2000 Water Vapor Intensive Operating Periods

The analysis of the results of ETL's participation in the 1997, 1998, and 2000 Water Vapor Intensive Operating Periods at the Southern Great Plains Central Facility [7] was published in the open literature. Previous results and publications are contained in the Progress reports of FY 2002 and FY2003**.** In addition, forward model studies in the 60 GHz spectral region, using data from the ARM Microwave Profiler (MWRP) [8], showed differences in computed brightness temperatures of up to 10 K when using the AER-developed Monochromatic Radiative Transfer Model (Monortm). These results were incorporated into an updated and validated version of Monortm (v2.11) [9].

### REFERENCES

[7] Revercomb, H. E., et al., "The ARM program's water vapor intensive observation periods: overview, initial accomplishments, and future challenges," *Bull. Amer. Meteorol. Soc*., 217-236, February, 2003.

[8] Cimini, D., E..R. Westwater, Y. Han, S. J. Keihm**,** R. Ware, F. S. Marzano, and P. Ciotti, "Atmospheric Microwave Radiative Models Study Based On Ground-Based Multichannel Radiometer Observations in the 20-60 GHz Band". Proc., 14th ARM Science Team Meeting, March 22-26, 2004, Albuquerque, New Mexico. Available At http://www.arm.gov/docs/documents/technical/conf_0304/Index.Html

[9] Cady-Pereira et al., "Monochromatic Radiative Transfer Model (Monortm): Recent Developments." Specialist Meeting on Microwave Remote Sensing, February 24-28, 2004, Rome.

### PUBLICATIONS

Cimini, D., E. R. Westwater, Y. Han, S. J. Keihm, **"**Accuracy of ground-based microwave radiometer and balloon-borne measurements during the WVIOP2000 field experiment.**"** *IEEE Trans. Geosci. Remote Sensing*, 41(11):2605-2615 Part 1, November 2003.

Cimini, D., E.R. Westwater, Y. Han, S. J. Keihm**,** R. Ware, F. S. Marzano, and P. Ciotti, "Atmospheric Microwave Radiative Models Study Based On Ground-Based Multichannel Radiometer Observations in the 20-60 GHz Band". Proc., 14th ARM Science Team Meeting, March 22-26, 2004, Albuquerque, New Mexico. Available at http://www.arm.gov/docs/documents/technical/conf_0304/Index.Html

Marchand, R., T. Ackerman, E. R. Westwater, S. A. Clough, K. Cady-Pereira, and J. C. Liljegren, **"**An assessment of microwave absorption models and retrievals of cloud liquid water

using clear-sky data**"**, *J. Geophys. Res. (Atmospheres)***,** 108(D24):Art. No. 4773, December 19, 2003.

## 2. The NSA/AAO 2004 Arctic Winter Water Vapor Experiment

The 2004 Arctic Winter Water Vapor Experiment was conducted at the NSA/AAO field site near Barrow, Alaska, from March 9 to April 9 2004. The major goal was to demonstrate that millimeter wavelength radiometers can substantially improve water vapor observations during the Arctic winter. Secondary goals included forward-model studies over a broad frequency range, demonstration of recently developed calibration techniques, the comparison of several types of *in situ* water vapor sensors, and the application of infrared imaging techniques. During this experiment, radiometers were deployed over a broad frequency range (22.235 to 400 GHz), including several channels near the strong water vapor absorption line at 183.31 GHz. These radiometers were supplemented by frequent radiosonde observations and other *in situ* observations, including several "Snow White" Chilled Mirror radiosondes. The radiometers deployed were also useful for measuring clouds during these cold conditions. Radiometers that were deployed include the Ground-based Scanning Radiometer (GSR) of NOAA/ETL, the MWR and the MWRP of ARM, and an infrared cloud imager (ICI) operated by Montana State University. In addition, all of the ARM active cloud sensors (radar and lidars) were operating.

### *2.1 The Ground-based Scanning Radiometer*

NOAA/ETL designed and constructed a multi-frequency scanning radiometer operating from 50 to 400 GHz. The radiometers are installed into a scanning drum or scanhead (see Figure 1). The GSR uses the sub-millimeter scanhead with 11-channels in the 50-56 GHz region, a dual-polarization measurement at 89 GHz, 7-channels around the 183.31 GHz water vapor absorption line, a dual-polarized channel at 340 GHz, and three channels near 380.2 GHz. It also has a 10.6 micrometer infrared radiometer within the same scanhead. All of the radiometers use lens antennas and view two external reference targets during the calibration cycle. In addition, each of the radiometers' design includes two internal reference points for more frequent calibration. The GSR instrument is a modification of the Circularly Scanning Radiometer that operated at the NSA/AAO site in 1999 [5]. A substantial improvement in radiometer calibration for ground observation in the Arctic environment has been achieved. Based on our experience from the 1999 IOP, a new set of thermally stable calibration targets with high emission coefficients was also designed, constructed, and deployed. The primary use of the instrument is to measure temperature, water vapor, and clouds, at cold (-20 to -55 °C) and dry (PWV < 5 mm) conditions. A schematic of the GSR is shown below in Figure 1. The beam widths of the GSR channels are 1.8 ° and can be averaged to given beam-widths that are consistent with the ARM MWRP (4.5 to 5.5 °). In addition, the ARM MWR and MWRP [3] were also operated. Figure 2 shows the instruments as they were deployed during the experiment. The channels of the MWR, in addition to providing temperature and humidity profiles, are also useful in forward model studies. A summary of primary instruments is shown in Table 1.

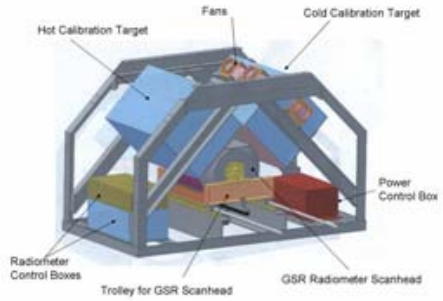


Figure 1. Schematic diagram of the Ground0based Scanning Radiometer (GSR) calibration and scanner system. The GSR scanhead periodically moves out of the framework for atmospheric viewing on a trolley system, and shares time observing the atmosphere and the two thermally controlled blackbody reference targets.


Figure 2. Photo of the deployments of the Microwave Profiler (MWRP), the Ground-based Scanning Radiometer (GSR), and the Microwave Radiometer (MWR) at the NSA/AAO during WVIOP04.

Table 1. Instruments deployed during the NSA/AAO Arctic Winter Radiometric Experiment

| Platform | Parameters Derived | Frequencies (GHz) |
|---|---|---|
| ARM MWR | PWV, ICL | 23.8, 31.4 GHz |
| GSR | PWV | 183.31 ± ( 0.5, ± 1, ± 3, ± 5, ± 7, ± 12, ± 15 GHz) |
| GSR | T, ICL | 50.3, 51.76, 52.625, 53.29, 53.845, 54.4, 54.95, 55.52, 56.025, 56.215, 56.325 GHz |
| ARM MWRP | T, PWV, ICL | 22.235, 23.035 ,23.835, 26.235, 30.000, 51.250, 52.280, 53.850, 54.940, 56.660, 57.290, 58.800 GHz |
| GSR | ICL | 89 GHz (dual-polarization) |
| GSR | PWV, ICL | 340 GHz (dual-polarization) |
| GSR | PWV, ICL | 380.2 ±4, ±9, ± 17 GHz |
| Infrared Cloud Imager | Spatial cloud coverage | 8-14 microns |
| GSR | Cloud presence | 10 microns |
| GPS | PWV | |
| Vaisala RS90 Radiosondes | T, P and ρ profiles | |
| Chilled Mirror Radiosondes | T, P and ρ profiles | |
| VIZ Radiosondes | T, P and ρ profiles | |

## *2.2 Preliminary Data*

### *2.2.1 Radiosondes*

During the experiment a number of radiosondes were launched. The ARM Operational Balloon Borne Sounding System radiosondes (BBSS) were launched daily at 2300 UTC at the Great White-the name of the site where ARM instruments are located. These BBSS systems used the Vaisala RS90 humidity elements. In addition, at the ARM Duplex, 1.4 miles to the west of the Great White, BBSS sondes were launched four-times daily (500, 1100, 1700, and 2300 UTC). Raw data from synoptic radiosondes from the National Weather Service (NWS) (1100 and 2300 UTC) were also archived. The NWS site is 4.3 km to the South-West of the Great White. Finally, during clear conditions, eight dual-radiosonde launches were launched by NASA at the ARM Duplex. For these releases, three during the day and five during the night, the Chilled Mirror "Snow White" radiosondes were attached to the same balloon that carried the BBSS sensor. In addition to the Chilled Mirror sensors, the NASA package also contained a Carbon Hygristor (CH) humidity sensor. For the month of the experiment, and after rigorous quality control to eliminate spurious data, a total of 196 soundings were available for analysis. Figure 3 shows one result when all systems were launched at the same time. Several features are evident from this figure. First, the temperature soundings from the instruments are in close agreement. Second, there are relatively small differences, of the order of 5% between the two Vaisala RS90 soundings and the Chilled Mirror. However, there were substantial disagreements between the CH soundings (NASA Hygristor and NWS AIR VIZ) and the other humidity measurements, above about 8 km. This anecdotal result was also shown in statistical comparisons as shown in Figure 4. We note a substantial bias in the humidity comparisons, with an average bias of about 5% below 10 km, but with a substantial increase to about 20 % above 8 km. Other statistical comparisons, not shown here, indicate that there was good agreement in humidity, of the order of 1 or 2 percent, between the Vaisala RS90 and Chilled Mirror sensors. As a final comparison, we show in Figure 5, the results of simultaneous humidity comparisons, on the same balloon, of the NASA Chilled Mirror (CM), the NASA Carbon Hygristor (CH), and the Vaisala RS90. Note the very poor agreement between the CM and the CH, again of the order of 20 % at higher altitudes, and the good agreement between the CM and the RS90. The evidence gives confidence that the humidity soundings made by the RS90 have high quality. We think that the availability of the 196 radiosondes in the 2004 experiment overcomes one of the principal limitations of the 1999 NSA/AAO experiment.

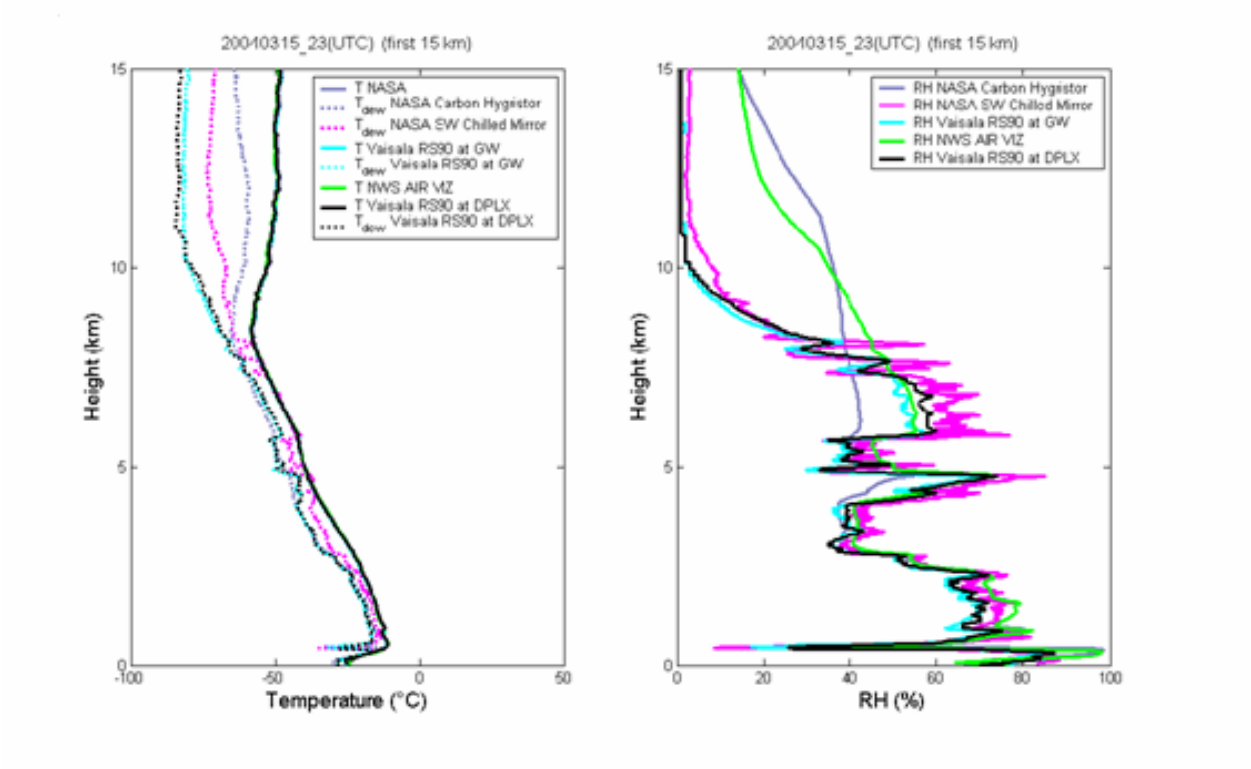


Figure 3. Comparisons of Radiosondes, including a dual-sonde launch, on March 15, 2004, at 2300 UTC, Barrow, Alaska.

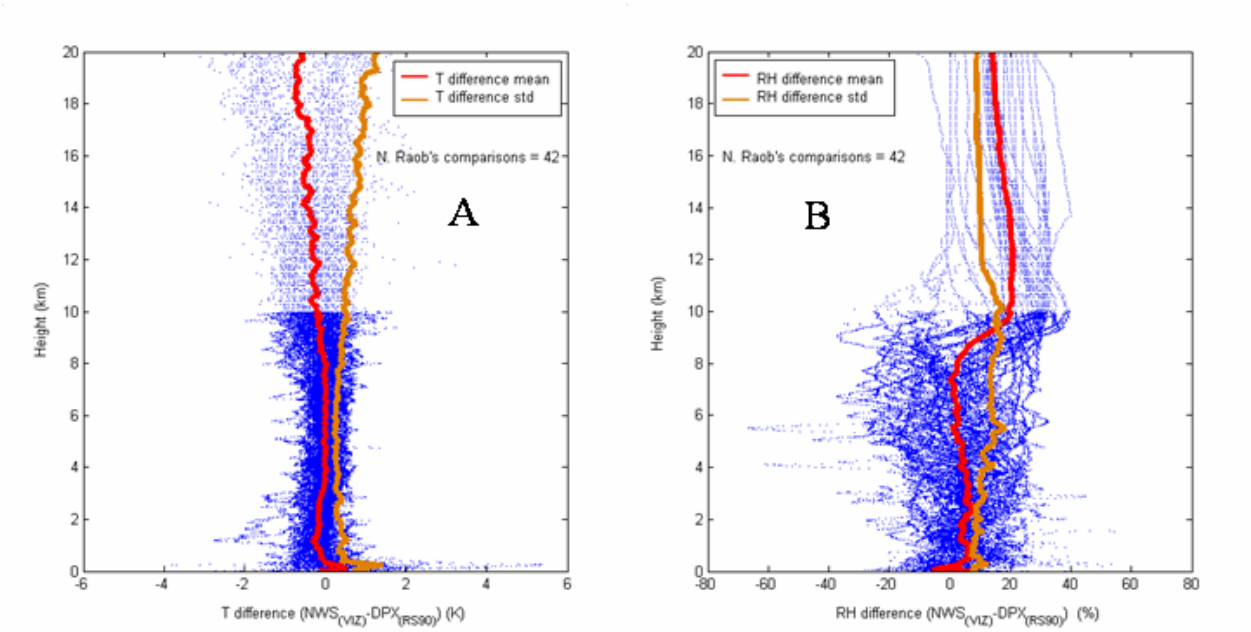


Figure 4. Statistical comparisons between NWS (Carbon Hygristor) and Duplex (Vaisala RS90) radiosondes. A: Temperature; B: Relative Humidity. Raw data were interpolated every 10 m below 10 km and every 100 m above 10 km.

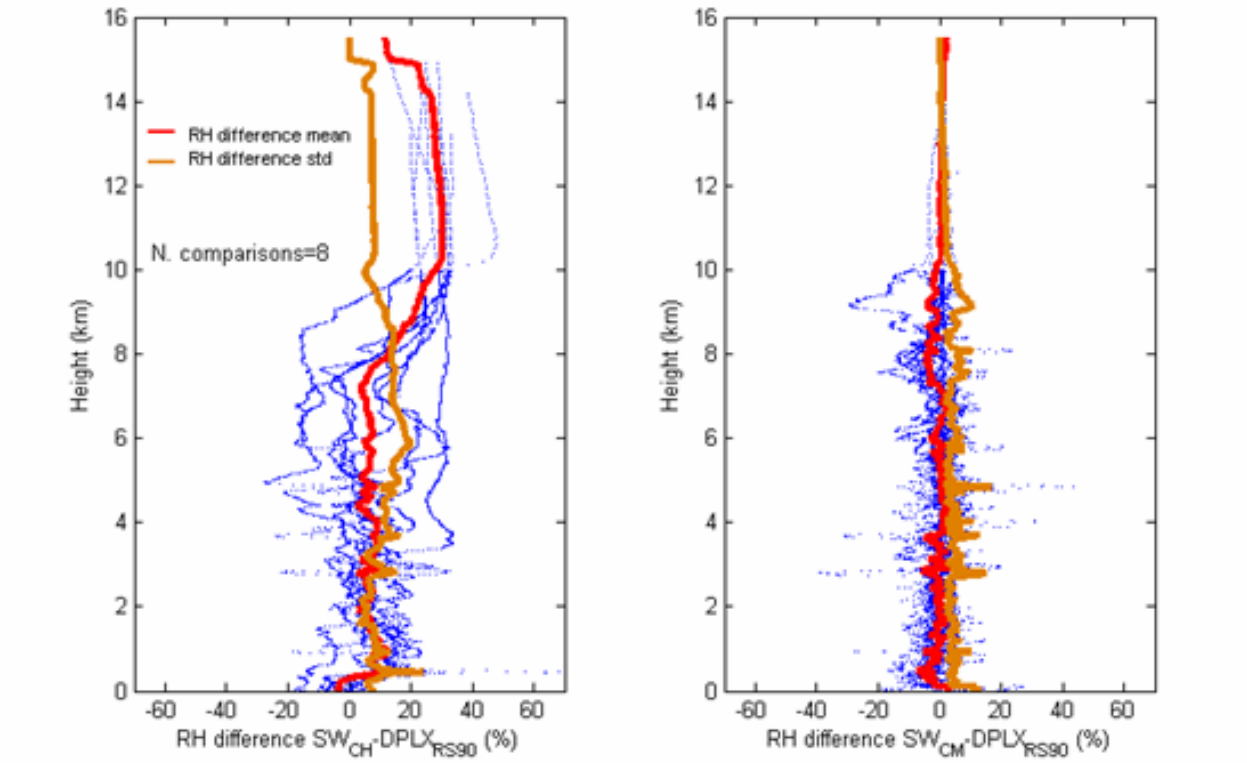


Figure 5. RH differences profiles between the NASA-launched Snow White Chilled Mirror ($SW_{CM}$) and Snow White Carbon Hygristor ($SW_{CH}$) and the Vaisala RS90 radiosondes. All sensors were on the same balloon that was launched at the ARM Duplex.

*2.2.2. Comparisons of MWR, MWRP, and Tb's calculated from BBSS radiosondes*

As discussed above, we launched Vaisala RS90 radiosondes from the ARM Duplex and from the Great White. As a preliminary evaluation of the quality of the data from the radiosondes, the MWR, and the MWRP, we compared the $T_b$ data measured by the two radiometers with $T_b$ calculated from the radiosondes, using the absorption algorithm of [13]. We note that the apparent problem with the NWS radiosondes appears in the MWRP channel at 22.235 GHz. This channel is known to be sensitive to upper altitude water vapor. The results, shown in Figure 6, are promising and a complete statistical analysis of the results will be done.

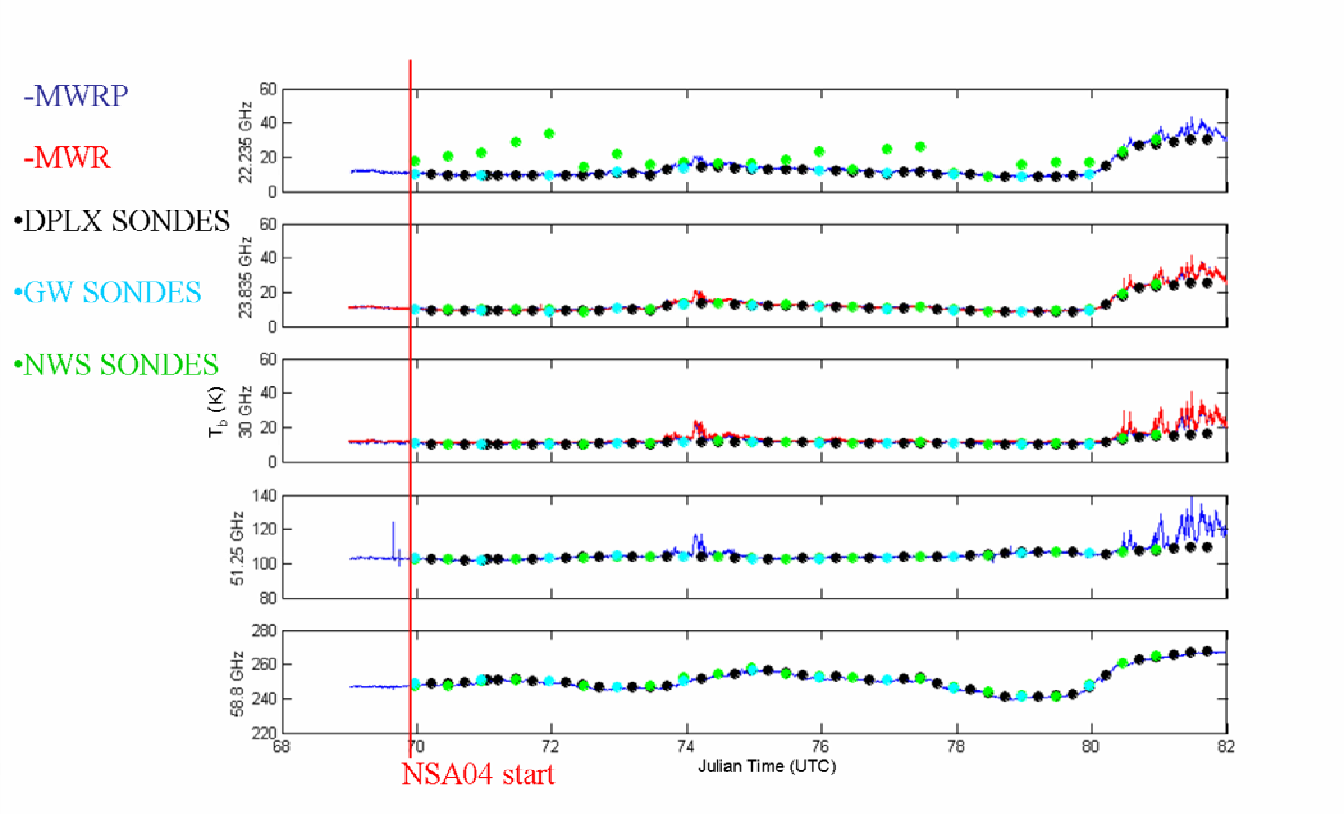


Figure 6. Comparison of $T_b$ measured by ARM radiometers with calculations based on BBSS and NWS radiosondes and the absorption model of [13].

*2.2.3. Typical target, continuous scan, and air-mass dwell for GSR.*

The GSR has a flexible and software programmable angular-scanning sequence that is repeated every two minutes. The sequence starts with the GSR being inside the calibration house and viewing the hot calibration target for 2 seconds. During the next step, the GSR remains in the calibration house and views the cold target, again for 2-seconds. The scanhead then moves out of the calibration house and moves to the atmospheric-scanning position, where it moves from air mass = 3.5 to a sequence of air mass dwells of 2-seconds each (air mass dwells at 3.5, 3.0, 2.5, 2.0, 1.5, 1.0). Between the air mass dwells the radiometer moves continuously to the next scan position. Thus the radiometer acquires both continuous and dwell data for the atmosphere with two-point calibration data in between. For channels in the transparency windows, both 2-point and tipcurve calibration methods can be used. In addition to the external calibration, the radiometer also switches between hot and cold internal calibration loads. Figure 7 shows the calibration sequence of the GSR.

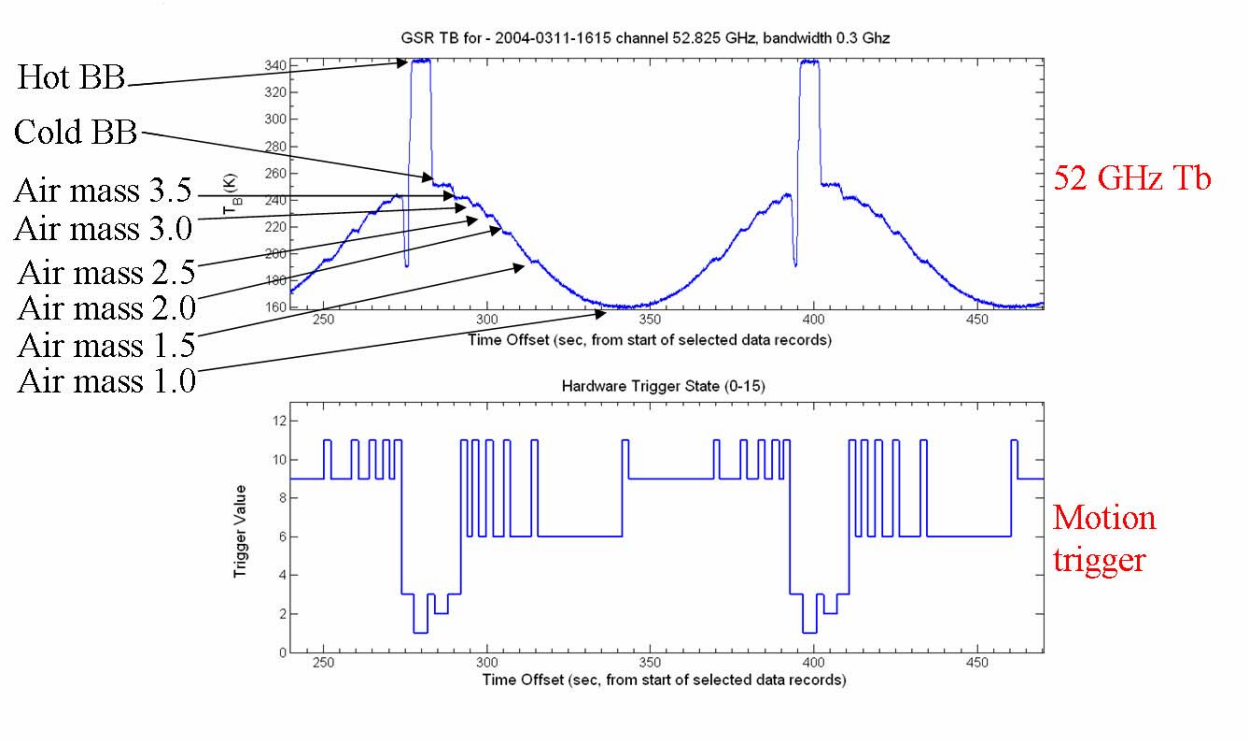


Figure 7. Calibration, dwell, and continuous scanning sequence of the GSR.

*2.2.4 Sample data from 50-60 GHz channels*

As shown in Table 1, the GSR takes data at 11 channels in the 50-60 GHz Oxygen band. In Figure 8, we show an eight-minute time series of data from these channels taken during the IOP. We note that the strongest channels from 55.5 to 56.3 GHz clearly show the presence of a thermal inversion, i.e., $T_b$ increases with increasing elevation angle. Conversely, the weakest channel at 50.3 GHz will allow tipcurve calibration. For all of the channels, the time spent dwelling at the separate air mass dwell points can be seen.

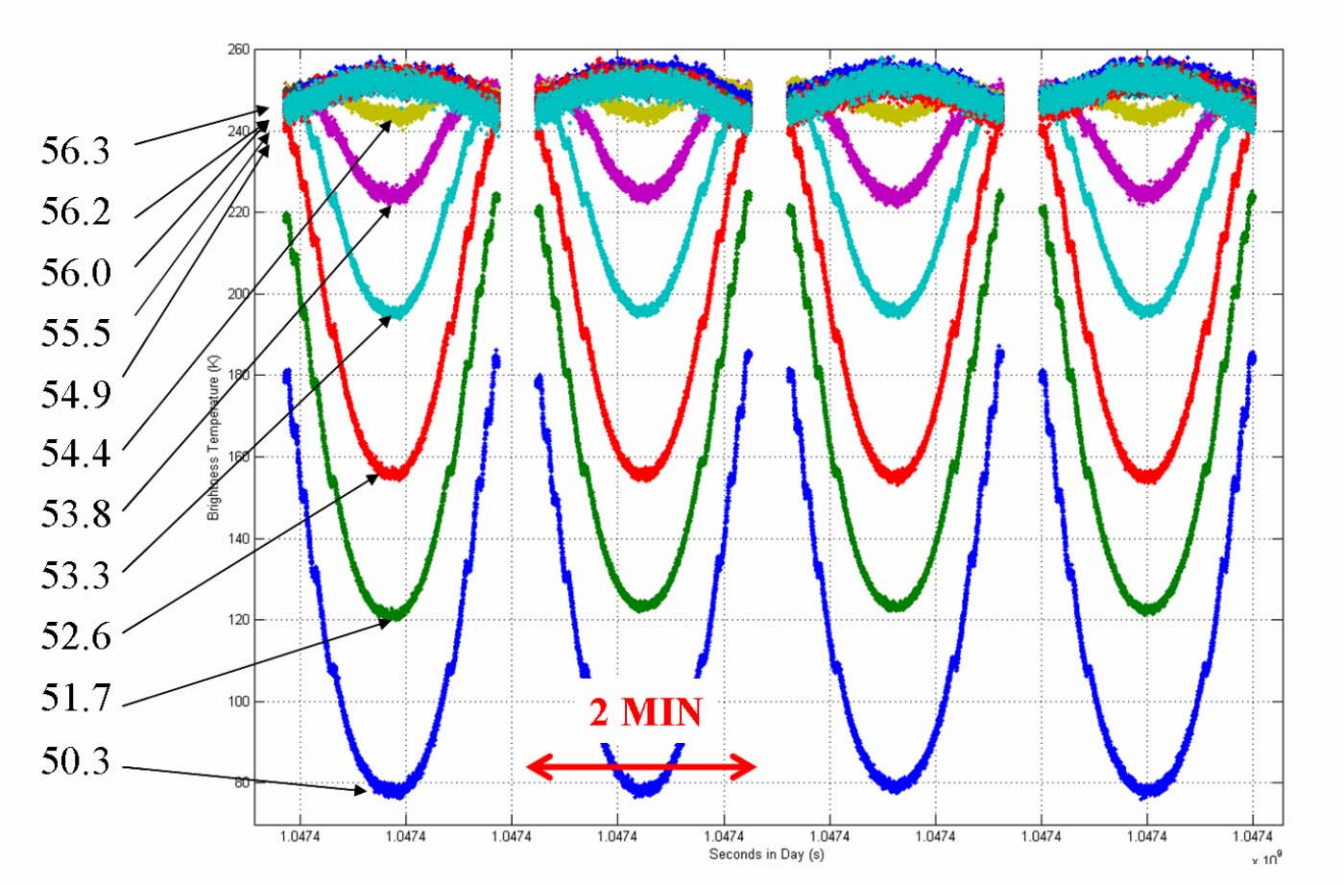


Figure 8. Time series of $T_b$ between 50 and 60 GHz. See Figure 7 for date and time of data.

### *2.2.5 Sample data from 183.31 GHz channels*

As shown in Table 1, the GSR takes data at 7 channels around the 183.31 GHz water vapor line. In Figure 8, we show a short series of data taken during the IOP. We note that the strongest channels from 183.31 ±0.5 and ±1 GHz are close to saturation; i.e., $T_b$ is close to the kinetic temperature of the atmosphere. Conversely, the weakest channels from 183.31 ± 15, ±12, and ±7 GHz all will allow tipcurve calibration. Again, for all of these channels, the time spent dwelling at the separate air mass dwell points can be seen.

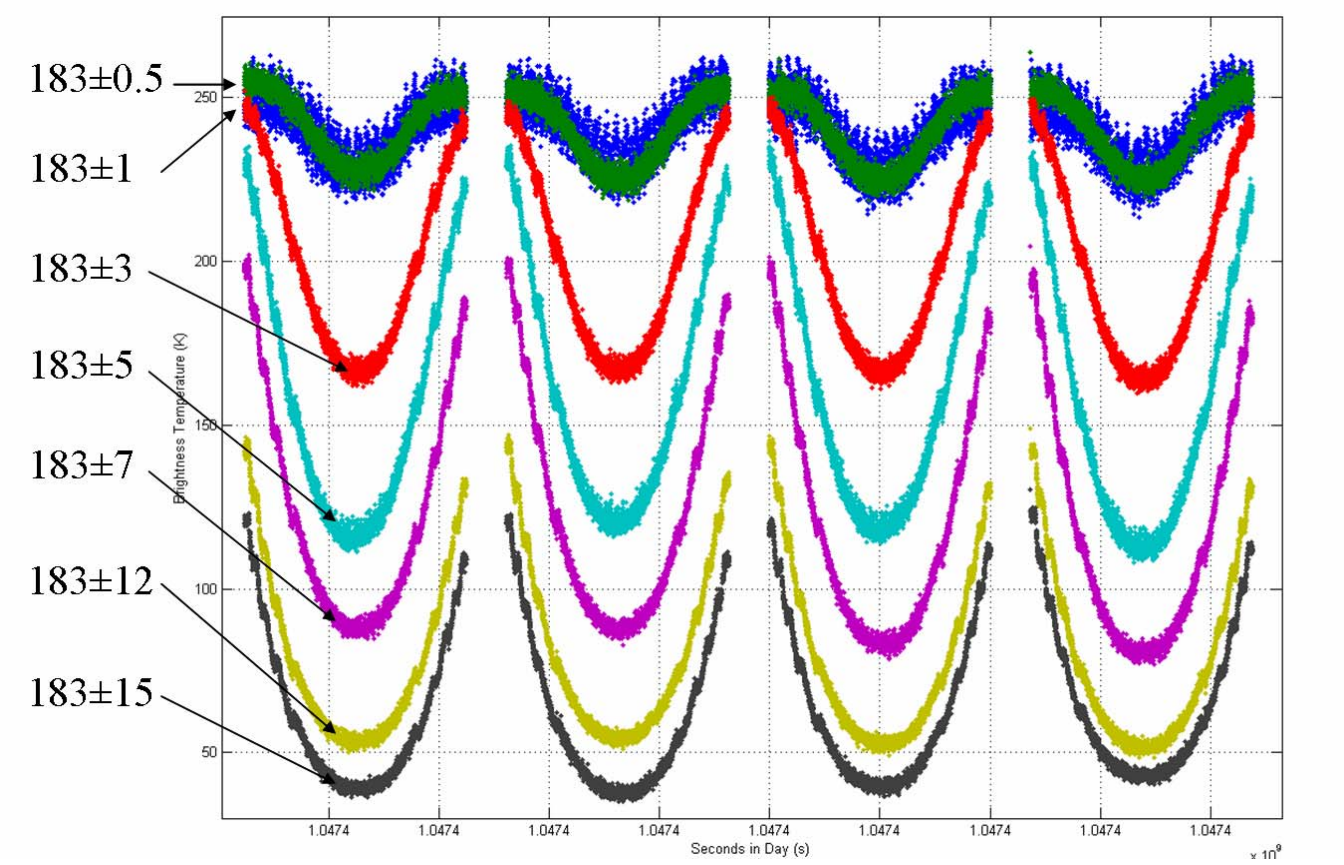


Figure 9. Time Series of $T_b$ for channels around the 183.31 GHz water vapor line. See Figure 7 for date and time of data.

### *2.3 Forward Model calculations for clear conditions*

In our analysis of both radiometer and radiosonde data, an important component will be to compare measurements and calculations of brightness temperature Tb. For a given radiosonde, and with the additional knowledge that the atmosphere is clear, Tb can be calculated as a function of frequency and angle from the Radiative Transfer Equation (RTE). The primary element in this equation is the absorption model that calculates the absorption coefficient for each radiosonde measurement of temperature T, relative humidity RH, and pressure P. In this work, we compare measurements of $T_B$ with calculations from three commonly used models: two were developed by Liebe and his colleagues [8]–[11] and the other by Rosenkranz [12], [13]. In addition we compared two models that were recently developed, one by Rosenkranz [13] and its modification by Liljegren et al. [3]. For convenience, we will refer to these models as LIEB87, LIEB93, ROS98, ROS03 and LILJ04. All of these models differ in the line-specific parameters such as line strength, self- and foreign-broadened line widths, as well as the so-called "continuum terms". The modification of [3] is associated with a 5% decrease in the self-broadened line width of the 22.235 GHz water vapor resonance. An example of a calculation is shown in Figure 10. It is evident that even between the two newer models [3] and [13]

significant differences occur. One of the primary goals of our continuing work will be to compare models with well calibrated measurements.

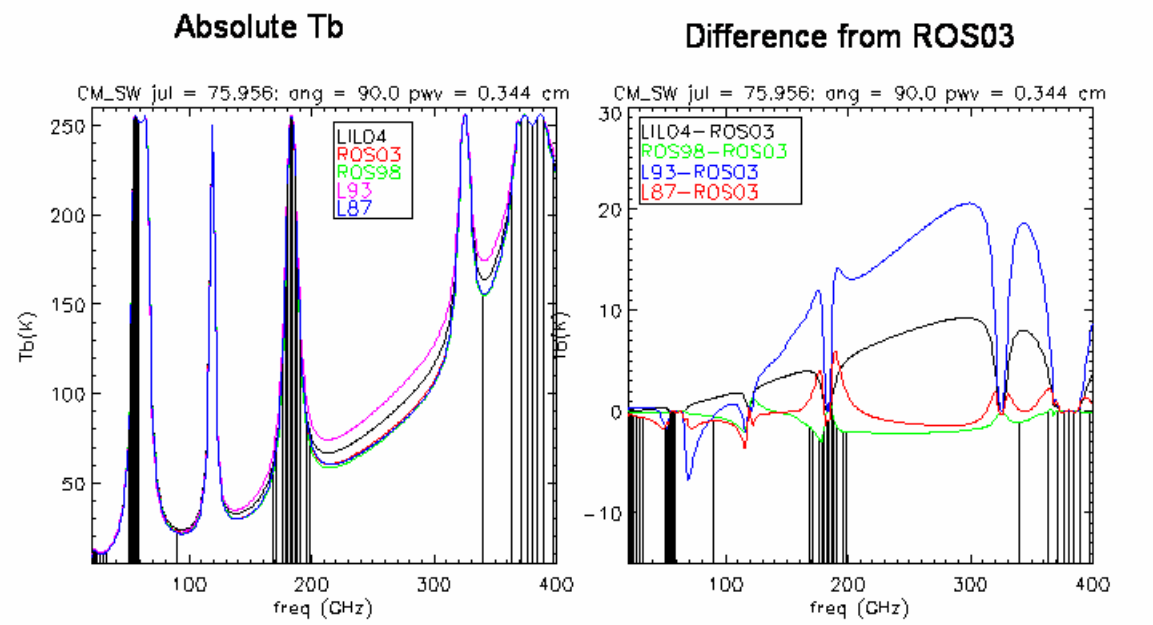


Figure 10. Comparisons of calculations of Tb using the five absorption models discussed in the text.

It is also of interest to compare, for a given absorption model, calculations of Tb for each of the various radiosonde measurements. An example of this type of calculation is shown in Figure 11. Although some differences exist between the Vaisala and the Chilled Mirror, differences of as much as 30 K appear with the Carbon Hygristor measurement.

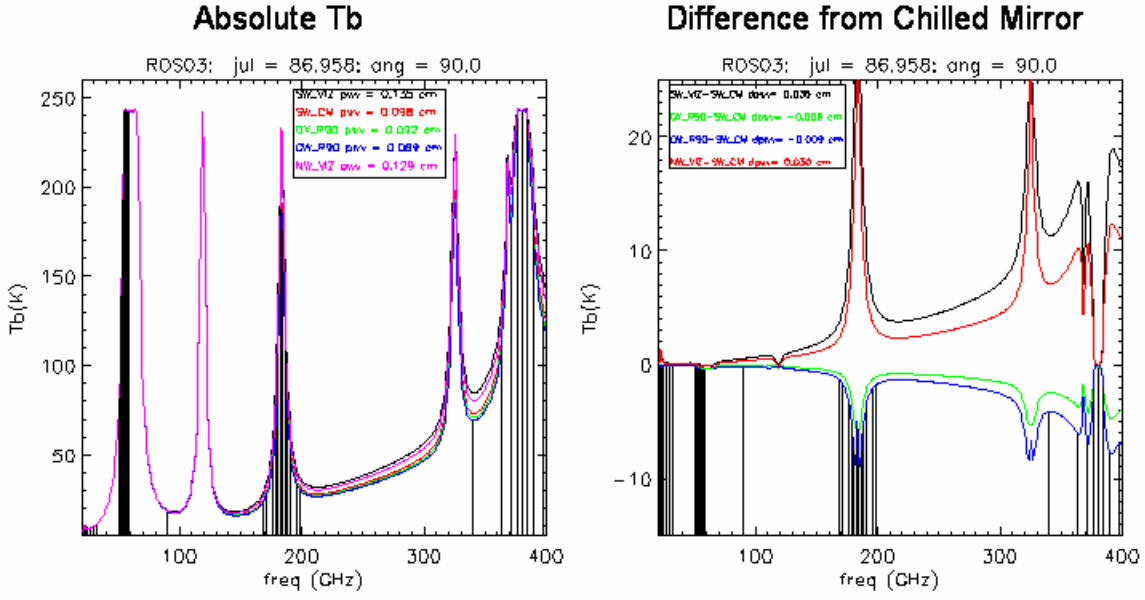


Figure 11. Comparison of calculations of Tb for the absorption model of Rosenkranz [13] and the five radiosondes mentioned in the text.

### *2.4 Forward model comparisons with the GSR*

Although the final calibrations of the GSR are not completed, some preliminary calculations that compare measured and computed Tb were done. The preliminary calibrations were based entirely on external target measurements that were made at the beginning and end of the elevation scans, and have not yet factored in possible gain changes that were made during scan. Nevertheless, as shown in Figure 12, there is qualitative agreement between the GSR measurements and the calculations based on [13]. We note again, that the calculations based on the NWS radiosondes may differ considerably with the other radiosondes and with the measurements.

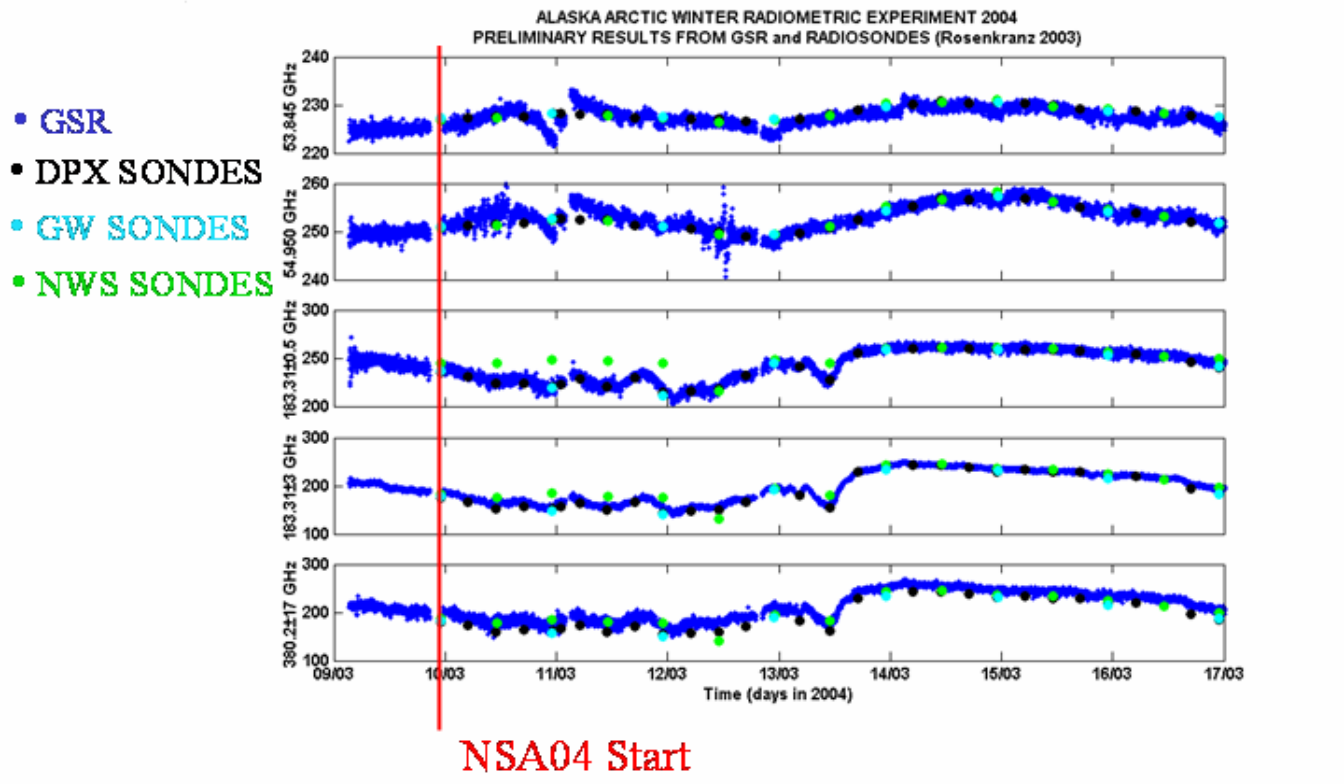


Figure 12. Comparison of Tb measurements by the GSR with calculations of Tb for the absorption model of Rosenkranz 2003 [13] and three of the five radiosondes mentioned in the text.

### *2.5 PWV comparisons between the MWR, GPS, and radiosonde calculations*

Measurements of PWV were made by the MWR (1 min temporal resolution), the MWRP, the GPS (30 min temporal resolution) that was co-located at the Great White, and the five radiosondes. Initially, there was substantial scatter in the GPS measurements due to ground

clutter and imprecise position information. A second reprocessing of the GPS data reduced some, but not all of the noise. A time series of the various PWV measurements is shown in Figure 13. As seen, there is good qualitative agreement between the measurements except below 0.5 cm, where the excess noise of the GPS is clearly evident. We also computed rms difference statistics of the various PWV measurements and these are shown in Table 2. Although the rms differences are about 0.5 mm, at the low end of the range of PWV, the percentage differences are substantial, and approach 50 %. Although an analysis of the MWR vs. MWRP is continuing, a preliminary comparison is shown in Figure 14. Again, although there is good qualitative agreement between the MWR and the MWRP, differences of 1 mm are present.

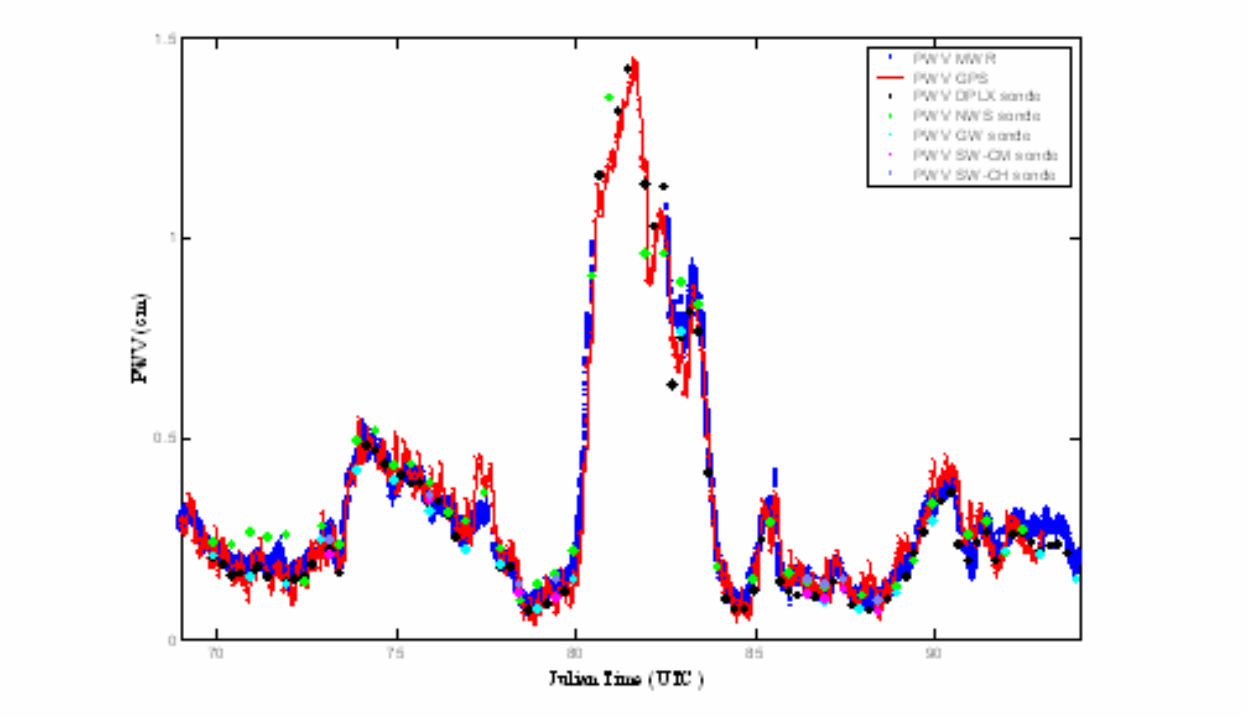


Figure 13. Comparison of PWV measurements by the GSR and the GPS with calculations from the five radiosondes mentioned in the text.

Table 2. Rms (cm) differences between MWR, GPS, and Radioondes

| | $DPLX_{(RS90)}$ sondes | $GW_{(RS90)}$ sondes | $NWS_{(VIZ)}$ sondes |
|---|---|---|---|
| MWR | 0.041 | 0.056 | 0.049 |
| GPS | 0.053 | 0.065 | 0.071 |

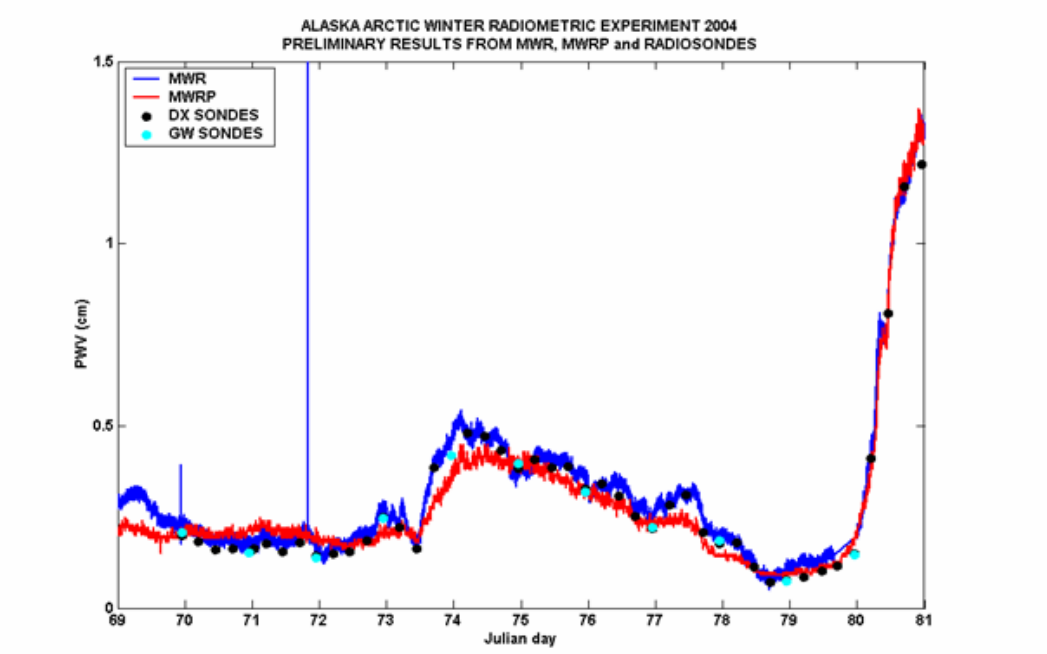


Figure 14. Comparison of PWV measurements by the MWR, the MWRP, and calculations from Vaisala RS90 radiosondes.

## References

[8] Liebe, H. J. and D.H. Layton, "Millimeter Wave Properties Of The Atmosphere: Laboratory Studies And Propagation Modeling," National Telecommunications and Information Administration (NTIA) Report 87-24, 1987, 74 pp. (available from the National Technical Information Service, 5285 Port Royal Road, Springfield, VA, 22161).

[9] Liebe, H. J., "MPM, An Atmospheric Millimeter Wave Propagation Model", *International J. Infra. Millimeter Waves*, vol.10, no. 6, pp. 631–650, 1989.

[10] Liebe, H. J., G.A. Hofford, and M.G. Cotton, "Propagation modeling of moist air and suspended water/ice particles and frequencies below 1000 GHz," *AGARD conference proceedings* 542, 3.1–3.10, 1993.

[11] Rosenkranz, P. W., "Water Vapor Microwave Continuum Absorption: A Comparison Of Measurements And Models," *Radio Sci.*, vol. 33**,** no. 4, pp. 919–928, 1998.

[12] Rosenkranz,P. W., Correction to "Water Vapor Microwave Continuum Absorption: A Comparison Of Measurements And Models," *Radio Sci.*, vol. 34, no. 4, p. 1025, 1999.

[13] Rosenkranz, P. W., Massachusetts Institute of Technology, Cambridge, MA, private communication, March 2003.

## PUBLICATIONS

Racette, P. E., E. R. Westwater, Y. Han, A. J. Gasiewski, M. Klein, D. Cimini, D. C. Jones, W.Manning, E. J.Kkim, J.R. Wang, V. Leuski, P. Kiedron, "Measurement of Low Amounts of Precipitable Water Vapor Using Ground-Based Millimeterwave Radiometry", *J. Atmos. Oceanic Technol.* (in press)

Westwater, E. R., M. Klein, A. Gasiewski, V. Leuski, J. Shaw, J. Liljegren,and B. M. Lesh, 2004: "The 2004 North Slope of Alaska Arctic Winter Radiometric Experiment", Proc. Microrad'2004. (ISSN 1824-2383)

Westwater, E. R., M. Klein, and V. Leuski, A. J. Gasiewsk, T. Uttal, and D. Hazen, D. Cimini , V. Mattioli , B. L. Weber, S. Dowlatshahi , J. A. Shaw , J. Liljegren ,B. M. Lesht , B. D. Zak; "The 2004 North Slope Of Alaska Arctic Winter Radiometric Experiment." Proc.14th ARM Science Team Meeting, March 22-26, 2004, Albuquerque, New Mexico. Available At http://www.arm.gov/docs/documents/technical/conf_0304/Index.Html

Westwater, E. R.. M. Klein, V. Leuski, A. J. Gasiewski, T. Uttal, D. A. Hazen, D. Cimini, V. Mattioli B. L. Weber, S. Dowlatshahi, J. A. Shaw, J. S. Liljegren , B. M. Lesht, and B. D. Zak, "Initial Results from the 2004 North Slope of Alaska Arctic Winter Radiometric Experiment", Proc. IGARSS'04

## 3. Day – night cloud statistics measured with the infrared cloud imager

Joseph A. Shaw
Department of Electrical & Computer Engineering
Montana State University
Bozeman, Montana 59717
ph. 406-994-7261; fax 406-994-5958; email jshaw@ece.montana.edu

Overview

Dr. Joseph Shaw's Optical Remote Sensing group at Montana State University has developed the Infrared Cloud Imager (ICI) for use in measuring spatial cloud statistics. We gained valuable experience operating the ICI system at the North Slope of Alaska (NSA) site in Barrow from February through May, 2002 and at the Southern Great Plains (SGP) site in Oklahoma during February – May 2003, as part of the Cloudiness Intercomparison Campaign (CIC). The ARM support for the project that is the subject of this progress report was used to develop algorithms for the ICI system, based on the previous deployment experiences and to employ those algorithms in analyzing data from the Arctic winter water vapor experiment at Barrow, Alaska in March – April 2004.

Accomplishments during Nov. 1, 2003 – Oct. 31, 2004

The key accomplishments during this past year include deploying the ICI system at the Arctic Winter Water Vapor Radiometry experiment in Barrow, Alaska during March – April 2004, and analyzing ICI data from the Cloudiness Intercomparison Campaign (CIC), held at the ARM SGP site during February – May 2003. The ICI is a thermal infrared imaging system that records radiometrically calibrated images of downwelling sky radiance in 320x240 pixels with a band-integrated wavelength range of 8-14 microns. The ICI data are spatially resolved but spectrally broad, which is a perfect complement to sensors such as AERI, whose data are at a single spatial point but resolved into many spectral bands.

The key advantage of the ICI over other cloud-imaging systems is that it performs cloud identification, cloud classification, and spatial-temporal cloud statistics with the same sensitivity and retrieval algorithm during both day and night. This is extremely important for the ARM program because of the need to produce data products with routine processing from data collected 24 hours per day, every day of the year. When we began the current ARM-funded project, the ICI system had not been used extensively in either Arctic or midlatitude locations, but during this funding period we have deployed the ICI at both SGP and NSA, generating a great amount of understanding of this and related cloud statistics measuring techniques. The data from the ICI are now being used not only to derive routine day-night cloud statistics, but also to help identify periods of partial cloudiness inside the microwave radiometer (MWR) antenna beam and to identify clear and cloudy periods for mm-wave radiometer analysis from the 2004 Barrow deployment.

Figure 15 is a photograph of the ICI system deployed near the GSR at the Great White facility at the North Slope of Alaska (NSA) site near Barrow, Alaska during March – April 2004. The ICI operated for over two months in harsh Alaskan weather without any user intervention, generating one sky image each minute during 24 hours each day, with a consistent radiometric calibration that was verified by comparison with Atmospheric Emitted Radiance Interferometer (AERI) data during periods of obviously clear or uniformly cloudy skies.

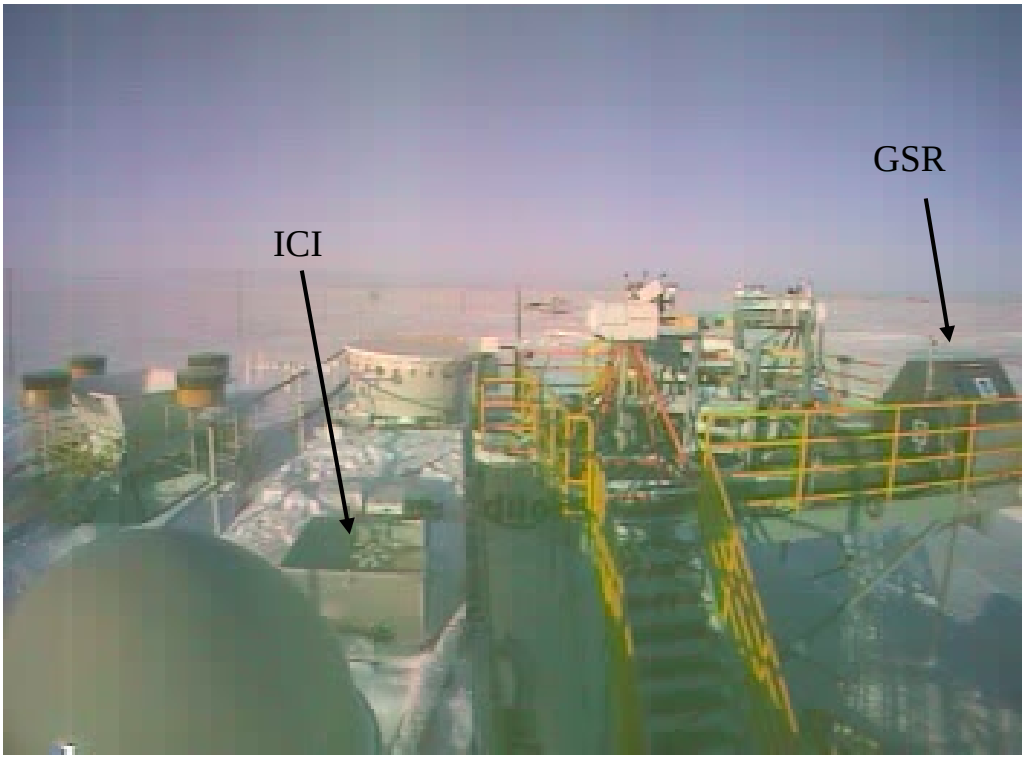


Figure 15. The Infrared Cloud Imager (ICI) system deployed at NSA, near the NOAA/ETL GSR system, during the Arctic Winter Water Vapor Radiometry experiment in March-April 2004.

The ICI generates images of the downwelling atmospheric radiance in the 8-14 μm thermal infrared band, with each pixel representing a radiance value (W/(m$^2$ sr). We often display ICI images in units of brightness temperature for the convenience of many users who prefer this; however, all data analysis is conducted in terms of radiance. Figure 16 is an example image from the ICI, showing thin cirrus clouds at night in Barrow, Alaska on March 9, 2004 during the Arctic Winter Water Vapor Radiometry experiment. This image illustrates the high radiometric contrast achieved by the ICI system even for thin cirrus. The brightness temperature is near -50$^o$C for the cirrus and near -80 $^o$C for the clear sky. Thicker and lower clouds are dramatically easier to sense with the ICI.

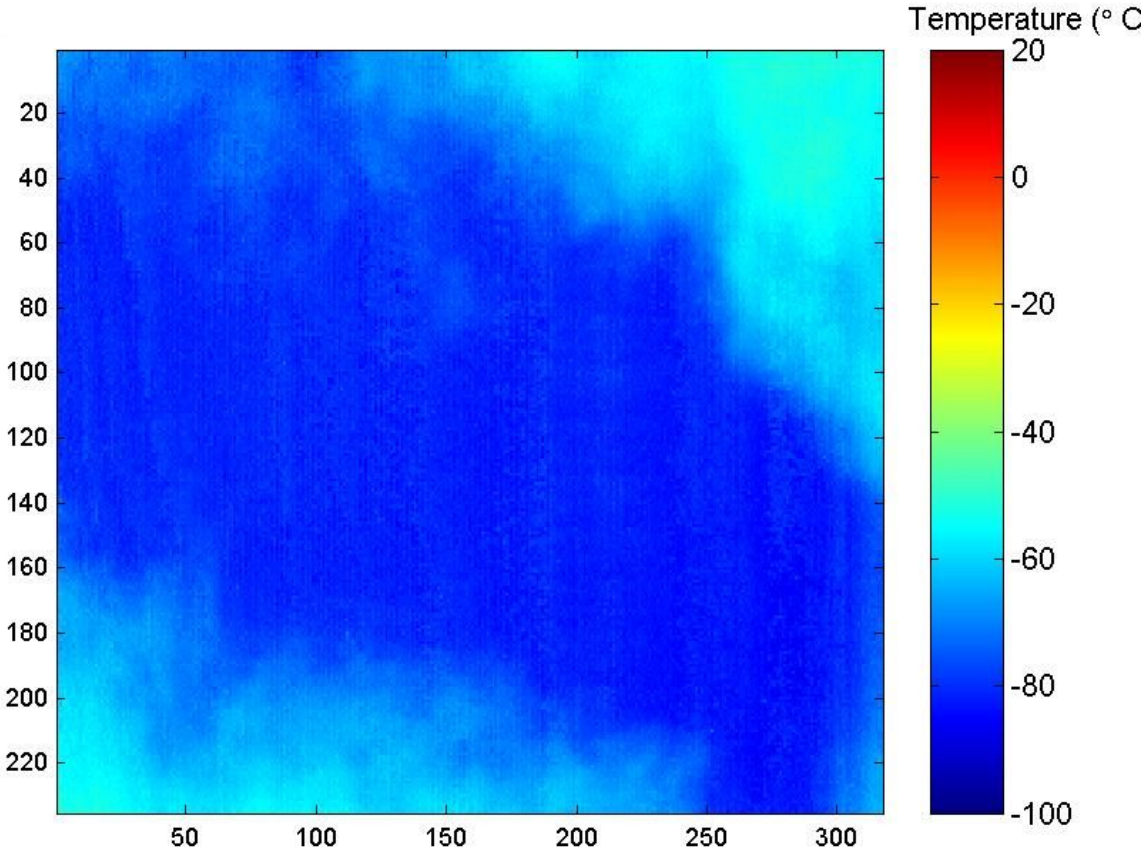


Figure 16. ICI image of nighttime clouds in Barrow Alaska at 0614UTC on March 9, 2004. Thin cirrus clouds at the bottom left and upper right have brightness temperature near -50$^o$C, while the clear sky in the center region of the image has brightness temperature near -80$^o$C.

Our analysis of the ICI data collected during the Cloudiness Intercomparison Campaign (CIC) at the SGP site in Oklahoma during February – April 2003 and during the Arctic Winter Water Vapor Radiometry experiment in Barrow, Alaska during March – April 2004 has answered several key questions that we set out to address in this effort. First was the issue of comparing cloud statistics obtained with zenith-pointing sensors and sky-imaging sensors. Cloud statistics often are obtained from zenith-pointing cloud lidars or radars, which rely on the assumption that

temporal statistics at the zenith are equal to spatial statistics over a larger region of the sky. To avoid problems of comparing cloud statistics from different sensors, we instead compared cloud statistics from the center of the ICI images with statistics from the entire ICI images. Figure 17 shows scatter plots of one-pixel cloud amount on the vertical and full-image cloud amount on the horizontal from NSA (left) and SGP (right). Both plots show that zenith measurements underestimate cloudiness relative to the full images (correlation coefficients ~ 0.98 and bias ~ 8-10%).

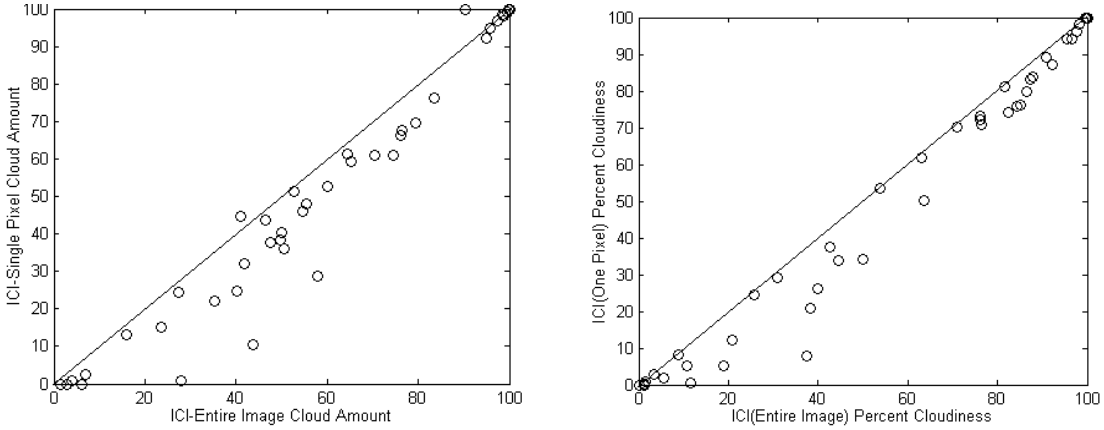


Figure 17. Scatter plots of ICI single-pixel and full-image cloud amount, illustrating that zenith measurements underestimate cloudiness. Data are from NSA (left) and SGP (right).

A similar, but much larger, bias was found in Whole Sky Imager (WSI) daytime and nighttime cloud amount measurements. Figure 18 shows scatter plots of WSI cloud amount on the vertical and ICI cloud amount on the horizontal for day (left) and night (right). These data are from the SGP site in Oklahoma during March-April 2003 at the Cloudiness Intercomparison Campaign (no WSI data were available when we had the ICI system deployed at the NSA site in 2004). During the daytime the two sensors agree reasonably well, with a correlation coefficient of 0.90 and rms difference of 18.0; however, at night the WSI strongly overestimates cloudiness relative to the ICI, with a correlation coefficient of 0.52 and an rms difference of 37.5. Scatter plots of ICI and micropulse lidar (MPL) data show consistent comparisons from both day and night (with good agreement, similar to that shown in Figure 17), which helps confirm that the ICI data are consistent during day and night, while the WSI data are strongly biased.

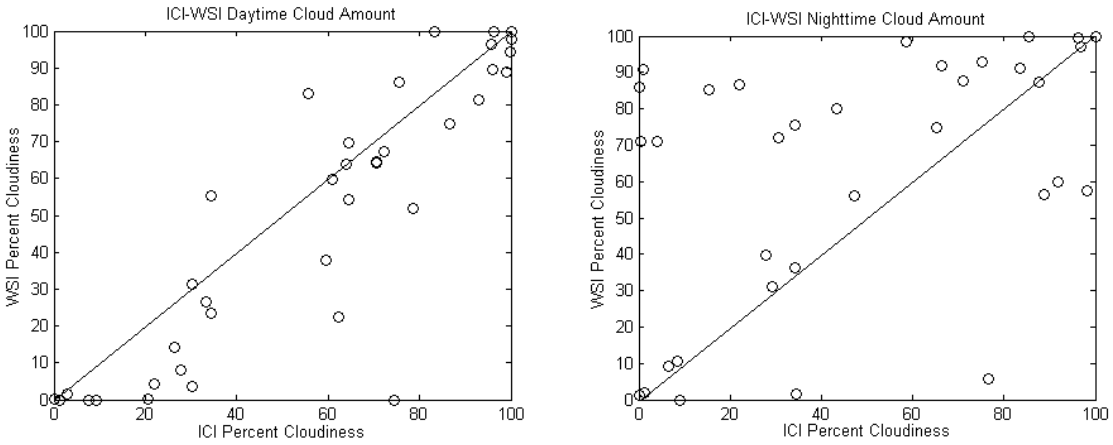


Figure 18. Scatter plots of Whole Sky Imager (WSI) and ICI cloud amount from the SGP site during day (left) and night (right), showing that the WSI's differing day and night algorithms create large biases and make it impossible to string together day and night data into a continuous time series. The ICI measures thermal atmospheric emission, which results in consistent day and night measurements.

The ICI data from NSA in March-April 2004 were passed through cloud-identification algorithms developed previously and cloud statistics for the entire experiment were obtained almost instantaneously. This is a huge improvement over previous processing, which relied on careful manipulation that took much longer periods of time. These data are now being applied to identifying clear and cloudy periods for mm-wave radiometer data analysis and for identifying periods when the microwave and mm-wave radiometer beams contained partial cloudiness.

**PUBLICATIONS**

Shaw, J. A. and B. Thurairajah, "Infrared Cloud Imager measurements of cloud statistics from the 2003 Cloudiness Intercomparison Campaign (CIC)," Proc. of the 14th ARM Science Team Meeting, March 22-26, 2004, Albuquerque, New Mexico. Available at: http://www.arm.gov/publications/proceedings/conf14/extended_abs/thurairajah-b.pdf

Shaw, J. A., B. Thurairajah, and K. Mizutani, "Cloud statistics measured with a ground-based infrared cloud imager," Proc. Of IGARSS'04, Anchorage, AK, Sept. 20-24, 2004.

Thurairajah, B., and J. A. Shaw, "Cloud statistics measured with the Infrared Cloud Imager," *IEEE Transactions on Geoscience and Remote* Sensing (submitted).

Thurairajah, B., "Thermal infrared imaging of the atmosphere: the Infrared Cloud Imager," M.S. Thesis, Dept. of Electrical and Computer Engineering, Montana State University, Bozeman, Montana, May 2004 (available online at http://www.montana.edu/etd/available/).

Shaw, J. A., B. Thurairajah, N. Pust, E. Edqvist, E. Mehiel, and K. Mizutani, "Radiometric sky imaging for cloud studies with a microbolometer-array infrared cloud imager," *Optics Express* (submitted).

## 4. Cloudiness Intercomparison Campaign

We participated in the 2003 Cloudiness Intercomparison Campaign (CIC) that was held at the SGP Central Facility in February-March 2003. Our efforts were mainly associated with analysis of data taken by three ARM Microwave Radiometers operating in continuous scanning modes. We also analyzed GSP soundings of water vapor and compared data of radiometers and GPS with radiosondes. The results were presented at ARM-sponsored workshops, at the ARM Science Team meeting, and were presented at an International Microwave Radiometry conference. We also did some forward model comparisons that are described below.

Brightness temperatures computed from five absorption models [3, 8-13]and Vaisala RS90 radiosonde observations were analyzed by comparing them with measurements from three microwave radiometers at 23.8 and 31.4 GHz. The radiometers were calibrated using two procedures, the so-called instantaneous "tipcal" method and an automatic self-calibration algorithm. Measurements from the radiometers were in agreement, with less than a 0.4-K rms difference during clear skies, when the instantaneous method was applied. Again, using the instantaneous method, brightness temperatures from the radiometer and the radiosonde showed a bias difference of less than 0.55 K when the most recent absorption models were considered. PWV computed from the radiometers were also compared to the PWV derived from a GPS station that operates at the ARM site. The instruments agree to within 0.1 cm in PWV retrieval. Figure 19 shows an example of our forward model comparisons [4].

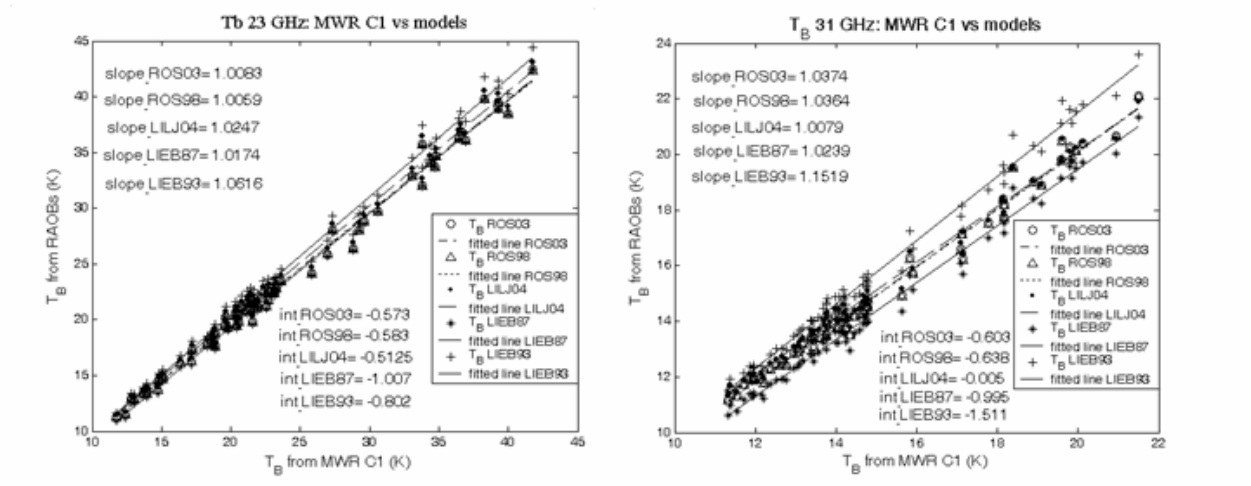


Fig.19(a) Fig.19(b)

Fig. 19. Scatterplots of $T_B$s from the MWR C1 (ARM calibration algorithm applied) versus $T_B$s computed from the RAOBs and the models LIEB87 (asterisks), LIEB93 (crosses), ROS98 (open triangles), ROS03 (white circles) and LILJ04 (black circles) during clear-sky conditions. The slopes and intercepts (int) of the regression line relative to the C1 measurements are also computed. Sample size is 67. (a) Scatterplot of $T_B$ at 23.8 GHz. (b) Scatterplot of $T_B$ at 31.4 GHz. After [4].

**PUBLICATIONS**

Mattioli, V., P. Basili, and E. R. Westwater, "Retrieval of Precipitable Water Vapor and Cloud Liquid Path by combining measurements from Scanning Microwave Radiometers and Global Positioning System". Proc. Microrad'2004. (ISSN 1824-2383).

Mattioli, V., and E. R. Westwater, "Precipitable Water Vapor and Cloud Liquid Path retrieval from Scanning Microwave Radiometer measurements during the 2003 Cloudiness Inter-Comparison Experiment". Proc. Microrad'2004 . (ISSN 1824-2383).

Mattioli, V., P. Basili, and E. R. Westwater, "Integration Of Global Positioning System And Scanning Water Vapor Radiometers For Precipitable Water Vapor And Cloud Liquid Path Estimates". Proc. 14th ARM Science Team Meeting, March 22-26, 2004, Albuquerque, New Mexico. Available at http://www.arm.gov/docs/documents/technical/conf_0304/index.html

Mattioli, V., E. R. Westwater, and V. Morris, "Monitoring Of Precipitable Water Vapor And Cloud Liquid Path From Scanning Microwave Radiometers During The 2003 Cloudiness Inter-Comparison Experiment". Proc. 14th ARM Science Team Meeting, March 22-26, 2004, Albuquerque, New Mexico. Available At http://www.arm.gov/docs/documents/technical/conf_0304/Index.Html.

Mattioli ,V., E. R. Westwater, S. I. Gutman, and V. R. Morris, "Forward Model Studies of Water Vapor using Scanning Microwave Radiometers, Global Positioning System, and Radiosondes during the Cloudiness Inter-Comparison Experiment", *IEEE Trans. Geosci. Remote Sensing* (in press).

Mattioli V., P. Basili, and E. R. Westwater, "Analisi Di Modelli Di Trasferimento Radiativo Tramite Radiometri A Microonde, Radiosonde E GPS. " XV RiNEm (Riunione Nazionale di Elettromagnetismo),Cagliari,Italy, 13-16 Settembre 2004

## 5. Atmospheric Profiling and Microwave Radiometry

We also contributed to several papers on atmospheric profiling and on new instruments and techniques in microwave radiometry. The publications are listed below.

**PUBLICATIONS**

Bianco, L., D. Cimini, F, Marzano, R. Ware and E. R. Westwater, "Improved Humidity Profiling By Combination Of Passive And Active Remote Sensors At SGP." Proc. 14th ARM Science Team Meeting, March 22-26, 2004, Albuquerque, New Mexico. Available At http://www.arm.gov/docs/documents/technical/conf_0304/Index.Html.

Ware, R., D. Cimini, P. Herzegh, F. Vandenberghe, J. Vivekanandan, and E. Westwater, "Ground-Based Radiometric Profiling during Dynamic Weather Conditions." Submitted to *J. Appl. Meteorol.*

Westwater , E. R., S. Crewell, and C. Matzler, "Review of Surface-based Microwave and Millimeter wave Radiometric Remote Sensing of the Troposphere." Radio Science Bulletin of URSI, 2004 (in press).

Westwater, E. R., S. Crewell, and C. Mätzler, "Frontiers in Surface-based Microwave and Millimeter Wavelength Radiometry", Proc. IGARSS'04.

## 6. Summary

The principal activities of this three-year project were focused on improved temperature, water vapor, cloud liquid, and cloud amount retrievals at the NSA/AAO. To this end we planned, developed instruments for, and conducted an intensive operating period at the ARM field site near Barrow, Alaska. The radiometric data from this experiment have been delivered to ARM and have been placed in the ARM data archive (http://iop.archive.arm.gov/arm-iop/2004/nsa/wviop/westwater-gsr).
In addition, we have developed web sites that contain additional information on the experiment and the principal instrument of this experiment - the GSR. These sites are
http://www.etl.noaa.gov/programs/2004/wviop/
and
http://www.etl.noaa.gov/technology/gsr/.
We have also contributed several open literature and conference publications describing our work. The references to these publications are contained in the Progress Reports for 2002, 2003, and this year-2004.

The major results of our NSA/AAO Arctic Winter Radiometric Experiment and our participation in the 2003 Cloud Intercomparison Campaign (CIC) are

1. There were substantial differences between five contemporary absorption models in calculating brightness temperatures between 20 and 400 GHz. However, there are two promising new models [3] and [14] that are deserving of extensive intercomparisons.
2. In the NSA/AAO experiments, a variety of radiosondes types were launched, including the Vaisala RS90, the Carbon Hygristor, and the Chilled Mirror. There were substantial differences (up to 20 % ) between RS90 and CH sensors, especially above 10 km. However, differences between the Chilled Mirror and the RS90 were much smaller, less than 1 %.
3. Preliminary comparisons between the GSR and the two ARM instruments (MWR and MWRP) indicate that high quality data were obtained for all of them. Thus, a substantial amount of profile retrieval combinations can be based on these data.
4. The Infrared Cloud Imager (ICI) was used to demonstrate that zenith-pointing sensors, such as cloud lidars and radars, underestimate cloudiness by assuming that temporal statistics at one point are equivalent to spatial statistics over a larger region of the sky.
5. The Infrared Cloud Imager (ICI) also showed that the Whole Sky Imager (WSI), which relies on red-blue ratios during the day and star maps at night to derive cloud fraction, exhibits extremely large biases between day and night cloud statistics.

6. The ICI produced the first ever continuous day-night time series of cloud amount at the NSA site during the March – April 2004 Arctic Winter Water Vapor Experiment and generated spatial cloud amount from routine processing, thereby demonstrating the practicality of thermal infrared radiometric sky imaging for deriving Arctic cloud statistics. This is particularly important for studies of cloud liquid and water vapor in the Arctic, where identification of cloud presence and cloud amount is difficult during the long winter night.

Promising research topics that will be pursued by us, and hopefully other ARM investigators, include:

1. GSR calibration studies using the combination of external targets, internal targets, and tipping curves. This research is of particular relevance to ARM because of the frequent occurrence of extended cloudy conditions when tipping curves are not possible.
2. Forward model studies, particularly in the clear atmosphere, where contemporary absorption models and their improvements can be investigated. We believe that use of the RS90 soundings in developing forward model studies is justified.
3. The input to profile retrieval algorithms of well-calibrated brightness temperature measurements, as functions of both frequency and angle, has significant potential. The information content of many combinations should be thoroughly investigated.
4. The availability of millimeter and sub-millimeter radiometric measurements of clouds is quite intriguing. Coupled with active measurements of clouds from lidars and radars, cloud micro-physical characteristics may be determined.
5. Weighting-function analysis has shown that some of the channels of both the WMRP and the GSR are sensitive to upper-tropospheric and lower-stratospheric water vapor. It is possible that measurements from these channels could be used as a (A) quality control on radiosonde upper atmospheric measurements, and (B) to partially correct some of these measurements.
6. There were substantial percentage differences between PWV retrievals of the MWR and the MWRP, especially at PWV concentrations below 0.5 cm. The reason for these differences should be investigated.
7. Thermal infrared radiometric imaging should be applied routinely at ARM sites, particularly with accurate radiometric calibration that will not only identify the presence of clouds, but also will avoid the misclassification of fog, haze, or blowing snow as clouds, and will provide cloud brightness temperature data to aid in retrieving cloud microphysical properties. Recent ARM Science Team Meeting papers have identified a potential infrared emission signature of haze that could play a significant role in atmospheric energy balance, and this should be studied carefully with a combination of MWR, AERI, ICI, and near-range aerosol lidars.